



Published in final edited form as:

Auton Neurosci. 2009 October 5; 150(1-2): 104–110. doi:10.1016/j.autneu.2009.06.004.

Inhibition of RVLM Synaptic Activation at Peak Hyperthermia Reduces Visceral Sympathetic Nerve Discharge

Kimberley G. Hosking, Richard J. Fels, and Michael J. Kenney

Department of Anatomy and Physiology, Kansas State University, Manhattan, KS 66506

Abstract

Hyperthermia is an environmental stressor that produces marked increases in visceral sympathetic nerve discharge (SND) in young rats. The brainstem in rats contains the essential neural circuitry for mediating visceral sympathetic activation; however, specific brainstem sites involved remain virtually unknown. The rostral ventral lateral medulla (RVLM) is a key central nervous system region involved in the maintenance of basal SND and in mediating sympathetic nerve responses evoked from supraspinal sites. In the present study we tested the hypothesis that inhibition of RVLM synaptic activation at peak hyperthermia (internal body temperature, T_c , increased to 41.5°C) would affect heating-induced visceral sympathetic activation. Experiments were completed in chloralose-urethane anesthetized, baroreceptor-intact and sinoaortic-denervated, 3-6 month-old Sprague-Dawley rats. Bilateral inhibition of RVLM synaptic activation produced by muscimol microinjections (400 and 800 pmol) at 41.5°C resulted in immediate and significant reductions in peak heating-induced renal and splenic sympathoexcitation. Interruption of RVLM synaptic activation and axonal transmission by lidocaine microinjections (40 nmol) at 41.5°C produced significant reductions in hyperthermia-induced sympathetic activation to similar levels produced by RVLM muscimol microinjections. The total amount of SND inhibited by RVLM muscimol and lidocaine microinjections was significantly more during hyperthermia (41.5°C) than normothermia (38°C). These findings demonstrate that maintenance of sympathetic activation at peak hyperthermia is dependent on the integrity of RVLM neural circuits.

Introduction

Hyperthermia is an environmental stressor that produces marked changes in the level of efferent sympathetic nerve discharge (SND). Acute elevations in internal body temperature (T_c) decrease SND directed to the caudal ventral artery in anesthetized rats (Johnson and Gilbey, 1994), increase muscle SND in conscious humans (Crandall et al., 1999, Niimi et al., 1997), splanchnic SND in conscious rats (Kregel et al., 1994), and renal, splanchnic, adrenal, and splenic SND in young anesthetized rats (Kenney et al., 1995, Kenney et al., 1998, Kenney and Fels, 2002, Kenney and Fels, 2003). Acute hyperthermia also alters the SND bursting pattern, transforming cardiac-related SND bursts in baroreceptor-innervated young rats to a pattern that contains low-frequency, high-amplitude bursts (Kenney et al., 1998). The functional role of heating-induced alterations in SND regulation is supported by at least three findings. First, surgical ablation of the celiac ganglion increases the rate of heating and reduces heat tolerance

Correspondence to: Michael J. Kenney, PhD, Department of Anatomy and Physiology, Kansas State University, Coles Hall 228, Manhattan, KS 66506, Phone: 785-532-4513, Fax: 785-532-4557, Kenny@vet.k-state.edu.

Publisher's Disclaimer: This is a PDF file of an unedited manuscript that has been accepted for publication. As a service to our customers we are providing this early version of the manuscript. The manuscript will undergo copyediting, typesetting, and review of the resulting proof before it is published in its final citable form. Please note that during the production process errors may be discovered which could affect the content, and all legal disclaimers that apply to the journal pertain.

time during hyperthermia (Kregel and Gisolfi, 1989), demonstrating the importance of an intact visceral sympathetic innervation for thermal tolerance (Kregel and Gisolfi, 1989). Second, heating-induced SND pattern changes contribute to the sympathoexcitation as low-frequency SND bursts contain more activity than cardiac-related bursts (Kenney et al., 1998). Third, heating-induced sympathetic activation is important for maintaining blood pressure while providing increased blood flow distribution for heat dissipation (Kenney et al., 1998).

Forebrain neural circuits, including the preoptic anterior hypothalamic area, are known to be important thermointegrative centers of the central nervous system (Gordon and Heath, 1986, Hammel, 1968, Hellon, 1970). However, visceral SND responses to acute heating are similar in midbrain-transected and sham midbrain-transected rats (Kenney et al., 2000), and the full expression of SND responses to acute heating is not evident in cervical spinal cord-transected rats (Kenney et al., 2000). These results indicate that heating-induced activation of visceral SND is not dependent on intact neural connections between forebrain and brainstem neural circuits and that the rat brainstem contains the essential neural circuitry for eliciting visceral SND responses to hyperthermia (Kenney et al., 2000). However, brainstem sites involved in mediating visceral SND responses to heating are not well understood.

The rostral ventral lateral medulla (RVLM) is a brainstem region that plays a critical role in basal and reflex regulation of SND (Barman, 1990, Dampney, 1994, Dampney et al., 2003, Loewy, 1990, Strack et al., 1989, Sun, 1995, Sun, 1996). RVLM neurons project to sympathetic preganglionic neurons in the spinal cord (Barman, 1990, Dampney, 1994, Dampney et al., 2003, Loewy, 1990, Strack et al., 1989, Sun, 1995) and inactivation of RVLM neurons produced by discrete RVLM microinjections of muscimol or lidocaine substantially reduce basal levels of SND (Cao et al., 2004, Fontes et al., 2001, Horiuchi and Dampney, 1998, Schreihofer et al., 2000). RVLM neurons play a critical role in mediating the sympathetic neural component of the baroreceptor reflex (Dampney et al., 2003, Guyenet, 2006) and are involved in cardiovascular and SND responses to several interventions (Fontes et al., 2001, Horiuchi et al., 2004, Kiely and Gordon, 1994, Nakamura et al., 2008). However, despite the prominent contribution of the RVLM to SND regulation and the profound influence of acute heating on sympathetic nerve outflow, the role of the RVLM in mediating SND responses to increased T_c remains virtually unexplored. This is a significant omission for at least two reasons. First, little information is known about central mechanisms mediating SND responses to hyperthermia despite the fact that heat illness/stroke is characterized by sympathetic nervous system dysregulation and cardiovascular alterations (Huang et al., 2005, Kregel and Gisolfi, 1989, Kregel et al., 1988). Second, SND and cardiovascular responses to acute heating are altered in aged compared with young subjects (Kenney and Fels, 2002; Kenney and Fels, 2003, Minson et al., 1998), although mechanisms contributing to age-related alterations in SND regulation to heating remain unexplored. Establishing a role for the RVLM in mediating SND responses to heating in young rats may provide the experimental foundation for determining mechanisms mediating altered SND regulation to acute heat stress in aged rats.

In the present study we tested the hypothesis that inhibition of RVLM synaptic activation at peak hyperthermia would markedly affect heating-induced visceral sympathoexcitation in anesthetized rats. The effect of bilateral inhibition of RVLM synaptic activation produced by muscimol (GABA_A receptor agonist) microinjections on the level of renal and splenic SND was determined after increasing T_c to 41.5°C. Additional experiments were completed to determine the effect on SND of interrupting both synaptic and axonal transmission in the RVLM by bilateral microinjections of lidocaine (sodium channel blocker) at a T_c of 41.5°C.

Methods

General Procedures

The Institutional Animal Care and Use Committee approved the experimental procedures and protocols used in the present study and all procedures were performed in accordance with the American Physiological Society's guiding principles for research involving animals. Male Sprague-Dawley rats (300-350 grams) were obtained from Harlan Sprague Dawley Inc. (Indianapolis, IN). All rats were housed in 6 × 9 inch cages, received rat chow and water ad libitum, and were maintained in a 24°C room on a 12:12-h light-dark cycle. Anesthesia was induced by isoflurane (3%) and maintained during surgical procedures using isoflurane (1.5%-2.5%), α -chloralose (80 mg/kg, ip), and urethane (800 mg/kg, ip). A catheter was placed in the femoral vein for the intravenous administration of maintenance doses of α -chloralose (35-45 mg/kg/hr). Maintenance doses of urethane (200 mg/kg every 4 hours) were administered intraperitoneally. The trachea was cannulated with a polyethylene-240 catheter and rats were paralyzed with gallamine triethiodide (5-10 mg/kg iv, initial dose; 10-15 mg/kg/hr, maintenance dose) and artificially ventilated. Femoral arterial pressure and heart rate (HR) were recorded using standard procedures. Tc was measured with a thermistor probe inserted approximately 5-6 cm into the colon and was kept at 38.0°C during surgery by a temperature-controlled table.

To eliminate the influence of baroreceptor afferent feedback mechanisms that can alter SND responses of central origin, selected experiments were completed in sinoaortic-denervated (SAD) rats. Bilateral denervation of the aortic arch was completed by sectioning the superior laryngeal nerve near its junction with the vagus nerve and removing the superior cervical ganglion. Bilateral carotid sinus denervation was completed by removing the adventitia from the area of the carotid sinus bifurcation. Sinoaortic-denervations were completed several hours before initiation of experimental protocols. The coherence function relating arterial pressure to SND was used to demonstrate the efficacy of the denervation procedure (Kenney et al., 1998). Coherence analysis provides a measure of the strength of linear correlation of two signals as a function of frequency. The lack of coherence between arterial pressure and SND at the frequency of the HR demonstrated a complete sinoaortic denervation (Kocsis et al., 1990, Hirai et al., 1995).

Sympathetic Nerve Recordings

Activity was recorded biphasically with a platinum bipolar electrode after capacity-coupled preamplification (bandpass 30-3000 Hz) from the central end of cut or distally crushed renal and splenic sympathetic nerves. The left renal and splenic nerves were isolated retroperitoneally and nerve-electrode preparations were covered with silicone gel to prevent exposure to room air. The sympathetic nerve potentials were full wave rectified and integrated (time constant 10 ms) which produced a smooth tracing of the synchronized discharges. Total power in splenic and renal SND was quantified as volts × seconds (V·s) (Kenney et al., 1998) and SND recordings were corrected for background noise after administration of the ganglionic blocker, chlorisondamine (5 mg/kg iv).

RVLM Microinjections

Rats were placed in a stereotaxic apparatus, the incisor bar was set at -11 mm (Schreihofner et al., 2005), and the brainstem was exposed. As described by Ito and Sved (Ito and Sved, 1997), target stereotaxic coordinates for the RVLM were 1.6-2.0 mm rostral to calamus scriptorius, 1.7-2.1 mm lateral from midline, and 2.6-3.2 mm below the dorsal surface of the brain. RVLM microinjections were completed using multibarrel glass micropipettes (3 barrels, outside tip diameter 40-70 μ m) filled with appropriate drugs, with the pipette angled 20° rostrally (Schreihofner et al., 2005). Microinjection volumes were determined with the aid of

an operating microscope by measuring the displacement of the fluid meniscus in the micropipette barrel with respect to a horizontal grid. In the majority of experiments the RVLM was functionally identified by completing glutamate (1 nmol) (Schreihofer et al., 2005) microinjections across a range of coordinates to locate the RVLM site producing the largest increase in mean arterial pressure (MAP). RVLM sites producing glutamate-induced increases in MAP greater than 20 mmHg were selected as experimental sites. RVLM microinjection experiments were completed in 46 rats; glutamate mapping was completed in 24 of 25 baroreceptor-intact rats and 15 of 21 SAD rats.

Experimental Protocols

Before initiation of experimental protocols, anesthetized rats were allowed to stabilize for 60 min. At the end of this control period, Tc was increased at a rate of approximately 0.1°C/min from 38°C to 41.5°C using a heat lamp. End-tidal CO₂ was measured using a micro-capnometer (Columbus Instruments) and was maintained between 4.0% and 4.5% during experimental interventions by adjusting the frequency of ventilation during hyperthermia (control ventilatory rate, ~80-90 strokes/min; 41.5°C ventilatory rate, ~110-120 strokes/min). Five experimental protocols were completed. Microinjectate volume was 100 nl for each injection. 1) To determine the role of RVLM synaptic activation in sustaining visceral sympathoexcitation to hyperthermia, bilateral RVLM microinjections of muscimol were administered at a Tc of 41.5°C in baroreceptor intact (400 pmol, n=5; 800 pmol, n=3) and SAD (400 pmol, n=6; 800 pmol, n=4) rats. 2) To determine the effect of interrupting both synaptic and axonal transmission in the RVLM on SND activation to acute heating, bilateral RVLM microinjections of lidocaine (40 nmol) were completed at a Tc of 41.5°C in baroreceptor-intact (n=4) and SAD (n=5) rats. 3) Volume control experiments were completed by determining SND responses to bilateral microinjections of saline (100 nl) after Tc had been increased to 41.5°C in baroreceptor-intact (n=6) and SAD (n=4) rats. 4) Anatomical control experiments (n=5) were completed by determining SND responses to bilateral microinjections of muscimol and lidocaine (same doses as above) after Tc had been increased to 41.5°C into sites that failed to increase MAP in response to glutamate microinjections. Histological analysis revealed that anatomical control sites were typically dorsal or rostral to identified RVLM sites. 5) Temperature control experiments were completed by determining SND responses to bilateral microinjections of muscimol and lidocaine (same doses as above) at a Tc of 38.0°C (intact, n=9; SAD, n=5). Data included in the manuscript (MAP, HR, renal and splenic SND) were obtained at the following experimental times: 1) during the control period prior to initiation of heating, 2) at 0.5°C or 1.0°C increments as Tc was increased from 38°C to 41.5°C, and 3) each minute for three minutes after RVLM microinjections at 41.5°C. Data from temperature control experiments were obtained each minute for three minutes after RVLM microinjections at 38°C.

Brain Histology

At the end of each experiment, rats received an overdose of methohexital sodium (150 mg/kg, iv). Brains were removed and flash frozen in liquid nitrogen. Brains were frozen sectioned at 25 µm in the coronal plane using a cryostat and mounted on slides in serial sequence. The center of the injection site (as referenced to the tip of the micropipette) was localized by observing discrete clusters of latex microspheres. Microspheres could be observed in brightfield or epifluorescence (rhodamine filter cube: BP 515-560 excitation filter).

Data and Statistical Analysis

Values are means ± SE. Control values of SND were considered as 0% and renal and splenic SND data are expressed as percentage change from baseline. SND, MAP and HR responses were analyzed using analysis of variance techniques with a repeated-measures design followed by Bonferroni post hoc tests. The overall level of statistical significance was $p < 0.05$.

Results

Figure 1A shows the effect of a unilateral RVLM glutamate microinjection on arterial blood pressure from a representative experiment. The average increase in MAP to glutamate microinjections in right and left RVLM sites was similar within groups (baroreceptor-intact, right vs. left; SAD, right vs. left) (Figure 1B), but was higher in SAD compared with baroreceptor-intact rats (Figure 1B). Injection sites were verified by observing discrete clusters of latex microspheres that were injected from the micropipette. Figure 1C shows a representative example of brainstem histology and the location of microspheres in the RVLM. Figure 1D shows the distribution of RVLM injection sites mapped on a standard coronal section from the atlas of Paxinos and Watson (Paxinos and Watson, 2005) at the level 12.12 mm caudal to bregma. For display purposes every injection site is not shown; however, the centers of visualized injection sites were all in the RVLM and located within 200 microns of the represented section.

Figure 2 shows original tracings from a representative experiment of renal and splenic SND and arterial blood pressure recorded at control (38°C), during acute heating with Tc maintained at 41.5°C, during and immediately after bilateral RVLM muscimol (400 pmol) microinjections, 3 min after completion of RVLM microinjections, and following ganglionic blockade. SND (renal and splenic) recorded at 41.5°C was increased from levels recorded at 38°C. RVLM muscimol microinjections at 41.5°C produced immediate reductions in renal and splenic SND to levels below control and substantially reduced arterial blood pressure.

Tc was increased from 38°C to 41.5°C in 35 min and maintained at this level for 3 min after RVLM microinjections (Figure 3). Because similar results were observed between baroreceptor-intact and SAD rats (changes in renal and splenic SND recorded 3 min after RVLM microinjections of muscimol and lidocaine at 41.5°C in baroreceptor-intact and SAD rats are shown in Table 1), data from these groups were combined for presentation. The top panels of Figure 3 show summarized renal (left) and splenic (right) SND data from RVLM microinjections completed during acute heating. Renal (left) and splenic (right) SND were significantly increased from preheating control levels at 41.5°C. RVLM muscimol (400, n=11 pmol; 800, n=7 pmol) and lidocaine (40 nmol, n=9) microinjections at 41.5°C abruptly and significantly reduced renal and splenic SND from peak sympathoexcitatory levels for at least 3 min following the respective microinjections. Levels of SND recorded after RVLM microinjections did not differ between the doses of muscimol (400 and 800 pmol) or between muscimol (both doses) and lidocaine. Renal and splenic SND remained unchanged in response to RVLM saline (n=10) microinjections at 41.5°C.

The bottom panels of Figure 3 show summarized MAP (left) and HR (right) data from RVLM microinjections completed during acute heating. MAP was not substantially changed from control levels (38°C) during progressive hyperthermia. RVLM muscimol (400 and 800 pmol) and lidocaine (40 nmol) microinjections at 41.5°C abruptly and significantly reduced MAP. Levels of MAP recorded after RVLM microinjections did not differ between the doses of muscimol (400 and 800 pmol) or between muscimol (both doses) and lidocaine. MAP remained unchanged in response to RVLM saline microinjections at 41.5°C. HR was significantly increased from control levels during acute heating and bilateral RVLM microinjections of muscimol (400 and 800 pmol) and lidocaine (40 nmol) at 41.5°C produced significant but modest reductions in HR from peak heating levels. HR remained unchanged from peak heating levels in response to RVLM saline microinjections at 41.5°C.

Microinjection of muscimol with Tc maintained at 41.5°C into sites identified to be functionally outside the RVLM (non-RVLM, n=5) did not alter the level of SND (renal and

splenic combined for presentation) (Figure 4), whereas RVLM muscimol microinjection at 41.5°C (represented by 400 pmol data) significantly reduced SND (Figure 4).

Figure 5 shows summarized renal (left) and splenic (right) SND data from RVLM microinjection experiments completed at 41.5°C (same data as shown in Figure 3) and RVLM microinjection experiments completed at 38°C. RVLM muscimol (400 pmol, n=5; 800 pmol, n=4) and lidocaine (40 nmol, n=5) microinjections at 38°C significantly reduced renal and splenic SND below control levels. As shown previously, RVLM muscimol and lidocaine microinjections at 41.5°C significantly reduced renal and splenic SND from peak heating-induced levels, however, the percent reduction in SND from control levels following RVLM microinjections at 41.5°C was less than that observed following RVLM microinjections at 38°C.

Figure 6 shows summarized absolute levels (measured in volt•seconds, V•s) of renal (top) and splenic (bottom) SND from RVLM muscimol (400 and 800 pmol) and lidocaine (40 nmol) microinjections completed at 38°C (basal, left) and at 41.5°C (hyperthermia, right). SND data from RVLM muscimol (both doses) and lidocaine microinjections were combined for presentation. Control levels of renal and splenic SND were similar in each group. The amount of activity inhibited in response to RVLM muscimol and lidocaine microinjections was significantly greater during hyperthermia than normothermia for both renal SND (41.5°C, 16.8 ±1 V•s; 38°C, 7.9±1 V•s;) and splenic SND (41.5°C, 14. 8±2 V•s; 38°C, 8.5±1 V•s;).

Discussion

The current study revealed three new findings. First, bilateral inhibition of RVLM synaptic activation produced by muscimol microinjections at 41.5°C resulted in immediate and significant reductions in heating-induced renal and splenic sympathoexcitatory responses. Second, interruption of RVLM synaptic activation and axonal transmission by bilateral microinjections of lidocaine at 41.5°C produced significant reductions in hyperthermia-induced sympathetic activation to levels comparable to those produced by RVLM muscimol microinjections. Third, the total amount of visceral SND inhibited by RVLM muscimol and lidocaine microinjections was significantly greater during hyperthermia (41.5°C) than normothermia (38°C).

Determining a role for the RVLM in sympathetic nerve activation at peak hyperthermia required the completion of and interpretation of data from several experimental protocols. First, the RVLM was successfully targeted as demonstrated by completion of functional mapping procedures and histological analysis of RVLM anatomical sites. Consistent with previous findings by Schreihöfer et al. (Schreihöfer et al., 2005), RVLM glutamate microinjections significantly increased MAP in baroreceptor-intact and SAD rats, with pressor responses higher in SAD rats. Histological examination confirmed that the centers of the microinjection sites were contained in the rostrocaudal extent of the RVLM as described in the atlas of Paxinos and Watson (Paxinos and Watson, 2005). Second, muscimol microinjections at 41.5°C into sites that failed to increase MAP in response to glutamate microinjections had no effect on SND, demonstrating anatomical specificity of RVLM sites. Third, RVLM saline microinjections at 41.5°C had no effect on the level of SND, indicating that decreases in SND to RVLM muscimol and lidocaine microinjections during hyperthermia were not mediated by vehicle or volume effects. Fourth, RVLM muscimol and lidocaine microinjections produced similar reductions in SND in baroreceptor-intact and SAD rats, indicating that the arterial baroreflex did not play a key role in mediating the observed responses.

RVLM muscimol and lidocaine microinjections at 41.5°C reduced SND nearly 70% from peak heating-induced sympathoexcitation to levels ranging from slightly above to approximately

30% below preheating control values (Figure 5). Consistent with previous findings (Cao et al., 2004, Fontes et al., 2001, Horiuchi and Dampney, 1998, Schreihofner et al., 2000), RVLM muscimol and lidocaine microinjections at normothermia (38°C) reduced SND 60-70% below control values, suggesting at first glance that a similar amount of nerve activity was inhibited in response to RVLM microinjections completed at 38°C and 41.5°C. However, SND responses must be interpreted with caution when percent changes are calculated from markedly different levels, as is the case with SND recorded at 38°C and 41.5°C. Therefore, it was important to consider the effect of RVLM microinjections at 38°C and 41.5°C on the absolute level (measured as V*s) of renal and splenic SND. The total amount of nerve activity inhibited by RVLM muscimol and lidocaine microinjections was significantly greater during hyperthermia than normothermia for both renal and splenic SND (Figure 6), indicating that the functional integrity of RVLM neural circuits is required for sustaining a substantial component of visceral sympathetic activation recorded at peak hyperthermia.

Although RVLM muscimol and lidocaine microinjections at 41.5°C substantially reduced SND to below preheating control levels, the absolute level of activity remaining after RVLM microinjections was higher at 41.5°C than 38°C. Several possibilities can be considered to explain temperature-related differences in the level of SND remaining after RVLM muscimol and lidocaine microinjections. First, activation of RVLM sympathetic neural circuits during acute heating may be so profound that RVLM muscimol microinjections at 41.5°C did not sufficiently block synaptic activation. We considered this possibility and completed RVLM muscimol microinjections at two different doses (400 and 800 pmol), each of which produced similar reductions of SND. If the attenuated inhibition of SND after RVLM muscimol microinjections at 41.5°C was the result of insufficient block of RVLM synaptic activation, then it would be expected that dose-related differences in the level of inhibition would be evident, however this was not the case. Second, it may be that fibers of passage within the RVLM substantially contribute to sympathetic activation during acute heating. This is likely not the case, however, as similar levels of SND were recorded at 41.5°C after RVLM muscimol (both doses) and lidocaine microinjections. Third, in response to acute heating spinal neural systems can activate the sympathetic nervous system in the absence of supraspinal neural circuits (Kenney et al., 2000), suggesting that spinal sympathetic neural circuits may contribute to the higher level of SND remaining after RVLM muscimol and lidocaine microinjections in heated compared to nonheated rats. Fourth, visceral sympathoexcitation to acute heating may result from activation of neural circuits in the RVLM as well as in other brainstem regions. Consistent with this notion, the cell bodies of brainstem presympathetic neurons whose axons project to sympathetic preganglionic neurons in the spinal cord are located not only in the RVLM but also in the rostral ventromedial medulla, midline medulla, and the A5 cell group in the pons (Strack et al., 1989). Additionally, enhanced coupling between respiratory and sympathetic nerve-related central circuits may contribute to heat-induced visceral sympathoexcitation as hyperthermia enhances the frequency-domain coupling between SND and phrenic nerve bursts (Kenney et al., 1998). Fifth, it may be that RVLM neural circuits are not prominently activated during acute heating; rather, activation of neural circuits in other brainstem regions may increase the effectiveness of the basal excitatory drive arising from the RVLM, thereby enabling a modestly activated RVLM to drive a larger population of preganglionic sympathetic neurons.

Because heating-induced sympathoexcitatory responses play a critical role in mediating cardiovascular responses to increased T_c (Kenney et al., 1998, Kregel and Gisolfi, 1989, Kregel et al., 1988), it was expected that MAP would be altered following inactivation of the RVLM. RVLM muscimol and lidocaine microinjections at 41.5°C produced marked reductions in MAP to near or below 50 mmHg. Because of the profound hypotension produced by RVLM inhibition, we did not attempt to determine if RVLM muscimol and lidocaine pretreatment would prevent sympathoexcitatory responses to progressive hyperthermia. HR was

significantly increased during hyperthermia; however, bilateral inactivation of RVLM neural circuits at 41.5°C resulted in modest reductions in HR from peak heating-induced levels.

Determining the role of RVLM neural circuits in mediating visceral sympathoexcitation to acute hyperthermia is important for at least two reasons. First, although it is well established that the RVLM contains a diverse array of neurotransmitter and receptor systems (Sun, 1995) and that regulation of basal SND involves a complex balance between RVLM excitatory and inhibitory systems (Dampney, 1994, Dampney et al., 2003, Horiuchi et al., 2004, Ito and Sved, 1997, Kiely and Gordon, 1994, Sakima et al., 2000), much less information is known about RVLM regulatory mechanisms mediating SND responses to acute physiological stress. Because heating provides a potent stimulus to visceral SND and because a substantial amount of sympathetic activation during peak-hyperthermia is dependent on intact RVLM neural circuits, the current findings provide foundational information for designing studies to determine RVLM mechanisms mediating sympathetic activation to acute stress. For example, it may be that SND activation to heat stress is mediated by multiple receptor systems that interact in a dynamic and coordinated manner to produce profound enhancement of RVLM synaptic excitation and attenuation of synaptic inhibition. Second, the results of recent studies by Kenney and Fels (Kenney and Fels, 2002, Kenney and Fels, 2003) demonstrate attenuated SND activation to heating in aged rats. However, mechanisms contributing to age-related alterations in SND regulation to heating remain unexplored. It may be that aging modifies regulation of the RVLM in response to acute heating, for example, aging may shift the balance of RVLM regulation during heating to a state characterized by enhanced synaptic inhibition and reduced synaptic excitation.

Acknowledgments

This study was supported by National Heart, Lung and Blood Institute Grant HL-091342 (MJK) and a grant from the National Center for Research Resources, National Institutes of Health T32RR017497 (KGH).

References

- Barman, SM. Brainstem Control of Cardiovascular Function. In: Klemm, WR.; Vertes, RP., editors. *Brainstem Mechanisms of Behavior*. John Wiley & sons, Inc.; 1990. p. 353-81.
- Cao WH, Fan W, Morrison SF. Medullary pathways mediating specific sympathetic responses to activation of dorsomedial hypothalamus. *Neuroscience* 2004;126:229-40. [PubMed: 15145088]
- Crandall CG, Etzel RA, Farr DB. Cardiopulmonary baroreceptor control of muscle sympathetic nerve activity in heat-stressed humans. *Am J Physiol* 1999;277:H2348-52. [PubMed: 10600855]
- Dampney RA. Functional organization of central pathways regulating the cardiovascular system. *Physiol Rev* 1994;74:323-64. [PubMed: 8171117]
- Dampney RA, Horiuchi J, Tagawa T, Fontes MA, Potts PD, Polson JW. Medullary and supramedullary mechanisms regulating sympathetic vasomotor tone. *Acta Physiol Scand* 2003;177:209-18. [PubMed: 12608991]
- Fontes MA, Tagawa T, Polson JW, Cavanagh SJ, Dampney RA. Descending pathways mediating cardiovascular response from dorsomedial hypothalamic nucleus. *Am J Physiol Heart Circ Physiol* 2001;280:H2891-901. [PubMed: 11356650]
- Gordon CJ, Heath JE. Integration and central processing in temperature regulation. *Annu Rev Physiol* 1986;48:595-612. [PubMed: 3518621]
- Guyenet PG. The sympathetic control of blood pressure. *Nat Rev Neurosci* 2006;7:335-46. [PubMed: 16760914]
- Hammel HT. Regulation of internal body temperature. *Annu Rev Physiol* 1968;30:641-710. [PubMed: 4871163]
- Hellon RF. The stimulation of hypothalamic neurones by changes in ambient temperature. *Pflugers Arch* 1970;321:56-66. [PubMed: 5529742]

- Hirai T, Musch TI, Morgan DA, Kregel KC, Claassen DE, Pickar JG, Lewis SJ, Kenney MJ. Differential sympathetic nerve responses to nitric oxide synthase inhibition in anesthetized rats. *Am J Physiol* 1995;269:R807–13. [PubMed: 7485597]
- Horiuchi J, Dampney RA. Dependence of sympathetic vasomotor tone on bilateral inputs from the rostral ventrolateral medulla in the rabbit: role of baroreceptor reflexes. *Neurosci Lett* 1998;248:113–6. [PubMed: 9654355]
- Horiuchi J, Killinger S, Dampney RA. Contribution to sympathetic vasomotor tone of tonic glutamatergic inputs to neurons in the RVLM. *Am J Physiol Regul Integr Comp Physiol* 2004;287:R1335–43. [PubMed: 15271655]
- Horiuchi J, McAllen RM, Allen AM, Killinger S, Fontes MA, Dampney RA. Descending vasomotor pathways from the dorsomedial hypothalamic nucleus: role of medullary raphe and RVLM. *Am J Physiol Regul Integr Comp Physiol* 2004;287:R824–32. [PubMed: 15205184]
- Huang YP, Lin MT, Chen JS, Wu PY. Naltrexone protects against hypotension, hyperthermia, and beta-endorphin overproduction during heatstroke in rats. *J Pharmacol Sci* 2005;97:519–524. [PubMed: 15821338]
- Ito S, Sved AF. Tonic glutamate-mediated control of rostral ventrolateral medulla and sympathetic vasomotor tone. *Am J Physiol* 1997;273:R487–94. [PubMed: 9277530]
- Johnson CD, Gilbey MP. Sympathetic activity recorded from the rat caudal ventral artery in vivo. *J Physiol* 1994;476:437–42. [PubMed: 8057253]
- Kenney MJ, Barney CC, Hirai T, Gisolfi CV. Sympathetic nerve responses to hyperthermia in the anesthetized rat. *J Appl Physiol* 1995;78:881–9. [PubMed: 7775333]
- Kenney MJ, Claassen DE, Bishop MR, Fels RJ. Regulation of the sympathetic nerve discharge bursting pattern during heat stress. *Am J Physiol* 1998;275:R1992–2001. [PubMed: 9843889]
- Kenney MJ, Fels RJ. Sympathetic nerve regulation to heating is altered in senescent rats. *Am J Physiol Regul Integr Comp Physiol* 2002;283:R513–20. [PubMed: 12121865]
- Kenney MJ, Fels RJ. Forebrain and brain stem neural circuits contribute to altered sympathetic responses to heating in senescent rats. *J Appl Physiol* 2003;95:1986–93. [PubMed: 12882996]
- Kenney MJ, Pickar JG, Weiss ML, Saindon CS, Fels RJ. Effects of midbrain and spinal cord transections on sympathetic nerve responses to heating. *Am J Physiol Regul Integr Comp Physiol* 2000;278:R1329–38. [PubMed: 10801304]
- Kiely JM, Gordon FJ. Role of rostral ventrolateral medulla in centrally mediated pressor responses. *Am J Physiol* 1994;267:H1549–56. [PubMed: 7943401]
- Kocsis B, Gebber GL, Barman SM, Kenney MJ. Relationships between activity of sympathetic nerve pairs: phase and coherence. *Am J Physiol* 1990;259:R549–60. [PubMed: 2118732]
- Kregel KC, Gisolfi CV. Circulatory responses to heat after celiac ganglionectomy or adrenal demedullation. *J Appl Physiol* 1989;66:1359–63. [PubMed: 2708255]
- Kregel KC, Stauss H, Unger T. Modulation of autonomic nervous system adjustments to heat stress by central ANG II receptor antagonism. *Am J Physiol* 1994;266:R1985–91. [PubMed: 8024055]
- Kregel KC, Wall PT, Gisolfi CV. Peripheral vascular responses to hyperthermia in the rat. *J Appl Physiol* 1988;64:2582–8. [PubMed: 3403442]
- Loewy, A. Central Autonomic Pathways. In: Loewy, A.; Spyer, K., editors. *Central Regulation of Autonomic Functions*. Oxford University Press; New York: 1990. p. 28-43.
- Minson CT, Wladkowski SL, Cardell AF, Pawelczyk JA, Kenney WL. Age alters the cardiovascular response to direct passive heating. *J Appl Physiol* 1998;84:1323–1332. [PubMed: 9516200]
- Nakamura T, Kawabe K, Sapru HN. Cold pressor test in the rat: medullary and spinal pathways and neurotransmitters. *Am J Physiol Heart Circ Physiol* 2008;295:H1780–7. [PubMed: 18757476]
- Niimi Y, Matsukawa T, Sugiyama Y, Shamsuzzaman AS, Ito H, Sobue G, Mano T. Effect of heat stress on muscle sympathetic nerve activity in humans. *J Auton Nerv Syst* 1997;63:61–7. [PubMed: 9089540]
- Paxinos, G.; Watson, C. *The Rat Brain in Stereotaxic Coordinates*. Academic Press; San Diego, California: 2005.

- Sakima A, Yamazato M, Sesoko S, Muratani H, Fukiyama K. Cardiovascular and sympathetic effects of L-glutamate and glycine injected into the rostral ventrolateral medulla of conscious rats. *Hypertens Res* 2000;23:633–41. [PubMed: 11131276]
- Schreihof AM, Ito S, Sved AF. Brain stem control of arterial pressure in chronic arterial baroreceptor-denervated rats. *Am J Physiol Regul Integr Comp Physiol* 2005;289:R1746–55. [PubMed: 16123230]
- Schreihof AM, Stornetta RL, Guyenet PG. Regulation of sympathetic tone and arterial pressure by rostral ventrolateral medulla after depletion of C1 cells in rat. *J Physiol* 2000;529 Pt 1:221–36. [PubMed: 11080264]
- Strack AM, Sawyer WB, Hughes JH, Platt KB, Loewy AD. A general pattern of CNS innervation of the sympathetic outflow demonstrated by transneuronal pseudorabies viral infections. *Brain Res* 1989;491:156–62. [PubMed: 2569907]
- Sun MK. Central neural organization and control of sympathetic nervous system in mammals. *Prog Neurobiol* 1995;47:157–233. [PubMed: 8719915]
- Sun MK. Pharmacology of reticulospinal vasomotor neurons in cardiovascular regulation. *Pharmacol Rev* 1996;48:465–94. [PubMed: 8981563]

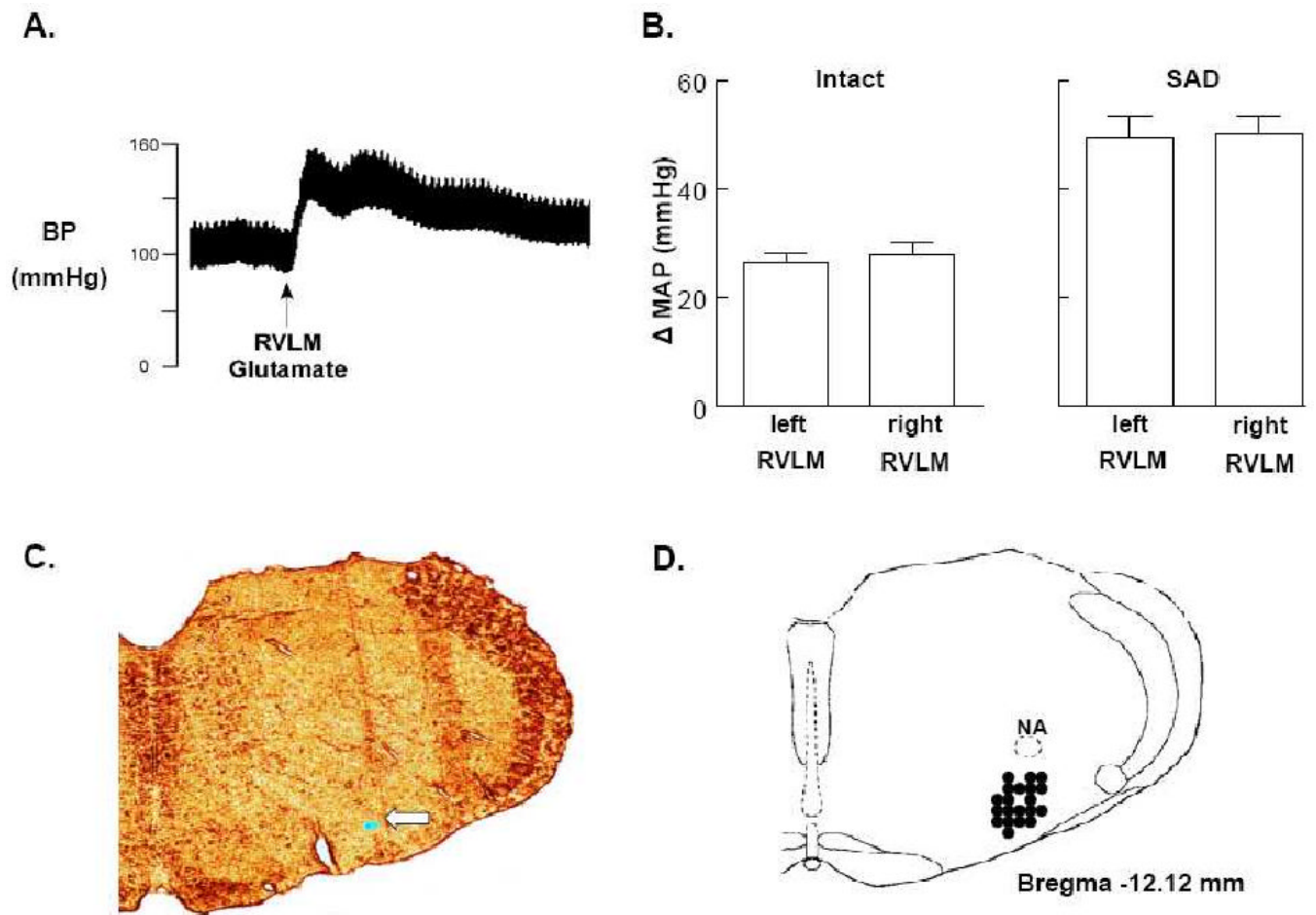


Figure 1.

A: Tracing of arterial blood pressure (BP) from a representative experiment completed before and after unilateral microinjection of glutamate into the RVLM. Horizontal calibration is 2 s. **B:** Average increases in MAP to glutamate microinjections in right and left RVLM sites in baroreceptor-intact (left) and sinoaortic-denervated (SAD) (right) rats. **C:** Representative histological coronal section of the medulla containing fluorescent microspheres (arrow) marking an RVLM microinjection site. **D:** Filled circles indicate the distribution of histologically verified RVLM microinjection sites mapped on a standard coronal section (Bregma -12.12 mm) from Paxinos and Watson (Paxinos and Watson, 2005).

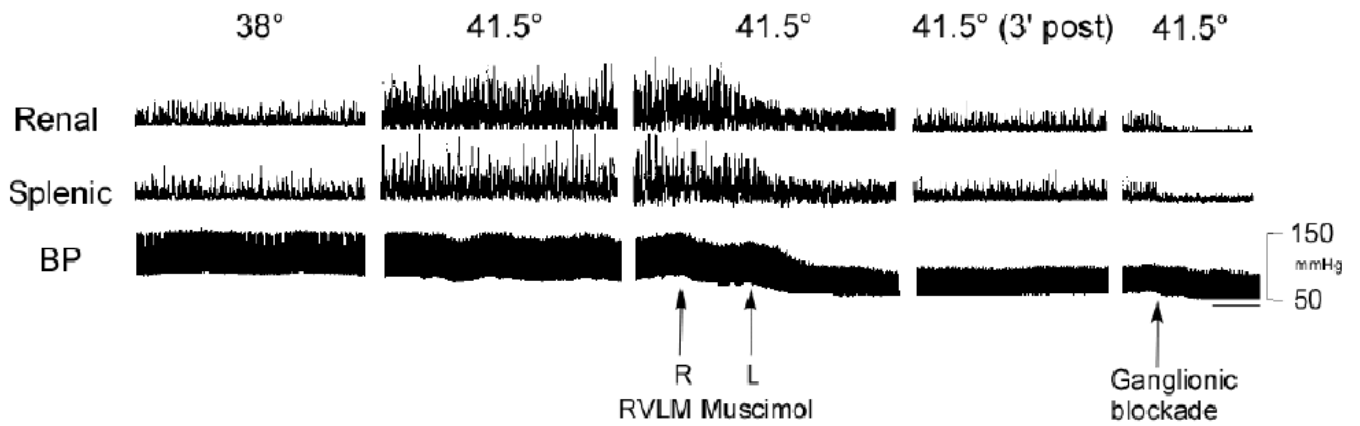


Figure 2.

Traces of integrated renal and splenic SND bursts and arterial blood pressure (BP) recorded at control (38°C), during acute heating with Tc maintained at 41.5°C, during and immediately after bilateral RVLM muscimol (400 pmol) microinjections, 3 min post-microinjection, and following ganglionic blockade. Horizontal calibration is 8 s.

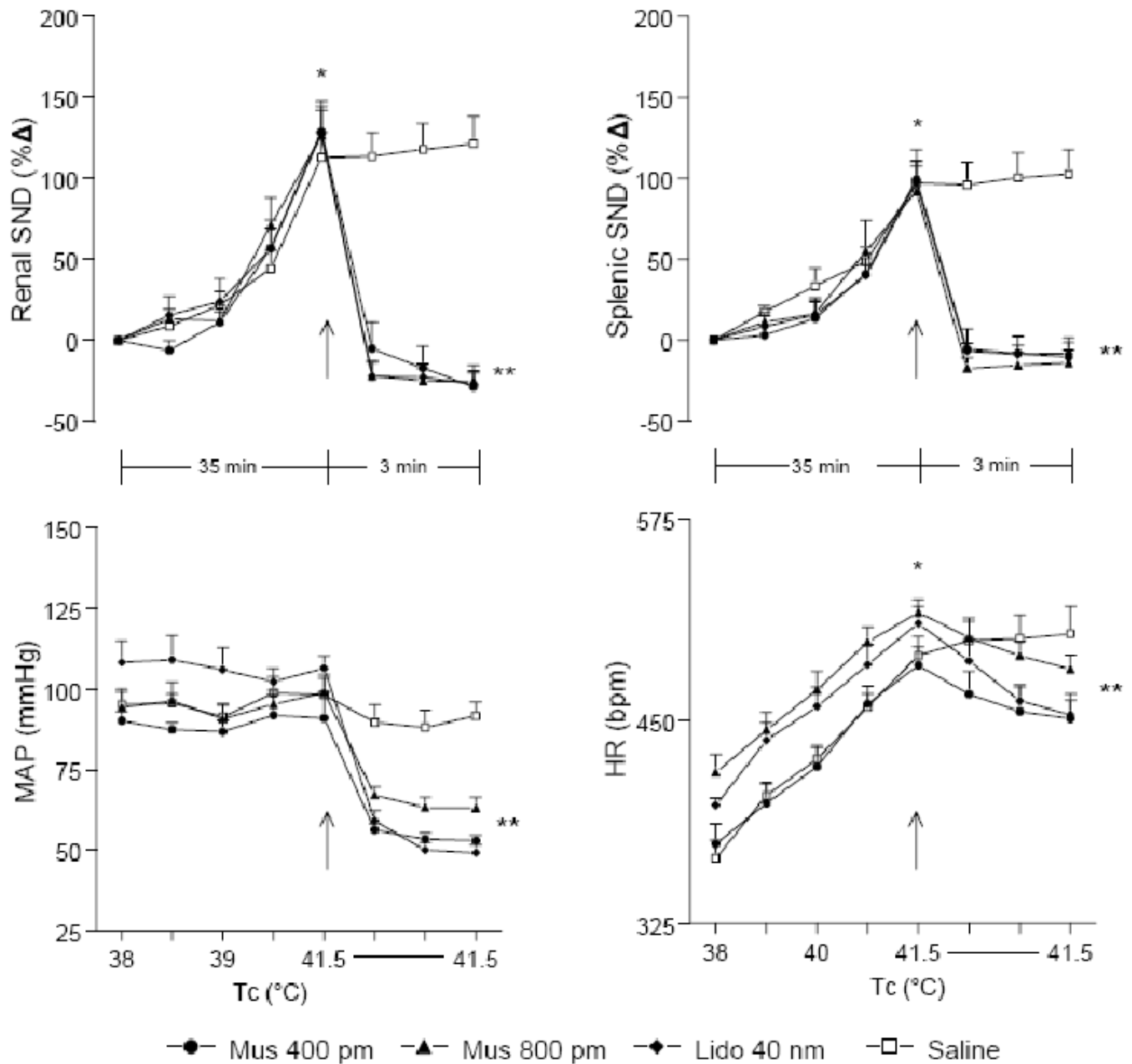


Figure 3.

Changes in renal SND, splenic SND, MAP, and HR during increases in Tc from 38° to 41.5° C and for 3 min following RVL microinjections (designated by arrow) of muscimol (400 pmol, n=11; 800 pmol, n=7), lidocaine (40 nmol, n=9), or saline (n=10) at 41.5°C. *Muscimol (400 and 800 pmol), lidocaine (40 nmol), and saline (100 nl) significantly different from control (38°C) at peak hyperthermia (41.5°C). **Muscimol (400 and 800 pmol) and lidocaine (40 nmol) significantly different from peak-heating levels at 1, 2 and 3 min post-microinjection.

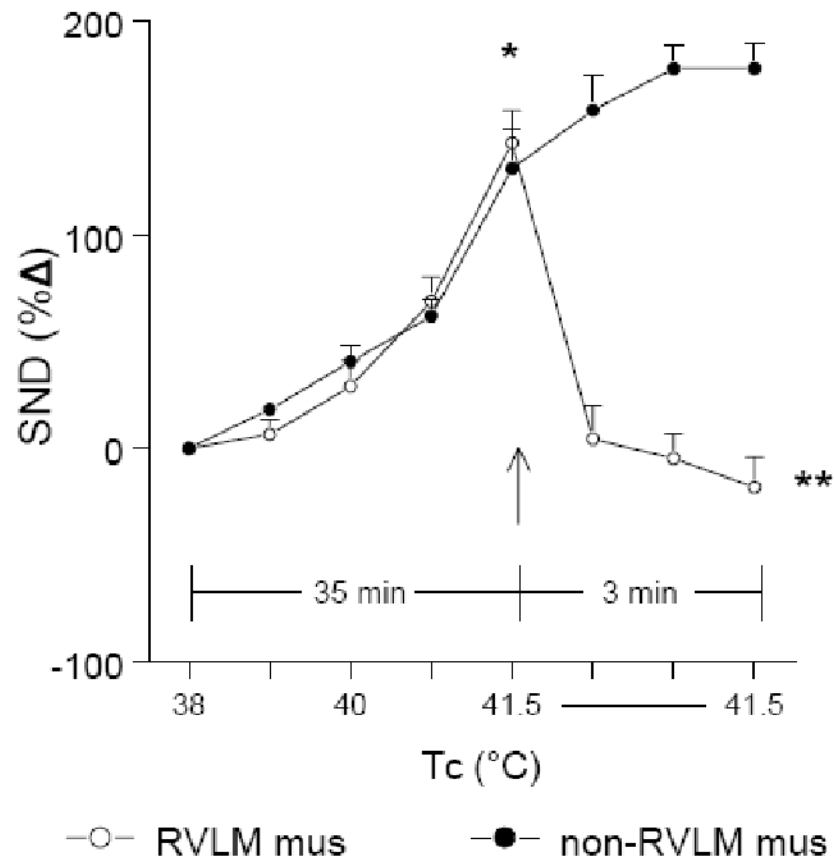


Figure 4.

Changes in renal and splenic SND (combined for presentation) during increases in Tc from 38° to 41.5°C and for 3 min following muscimol microinjections (Tc maintained at 41.5°C) in RVLM sites (RVLM mus, 400 pmol; open circles, n=11) and in sites identified to be functionally outside the RVLM (non-RVLM mus, 400 pmol; closed circles, n=5). *RVLM and non-RVLM microinjections significantly different from control (38°C). ** RVLM muscimol significantly different from non-RVLM muscimol at 1, 2 and 3 min post-microinjection.

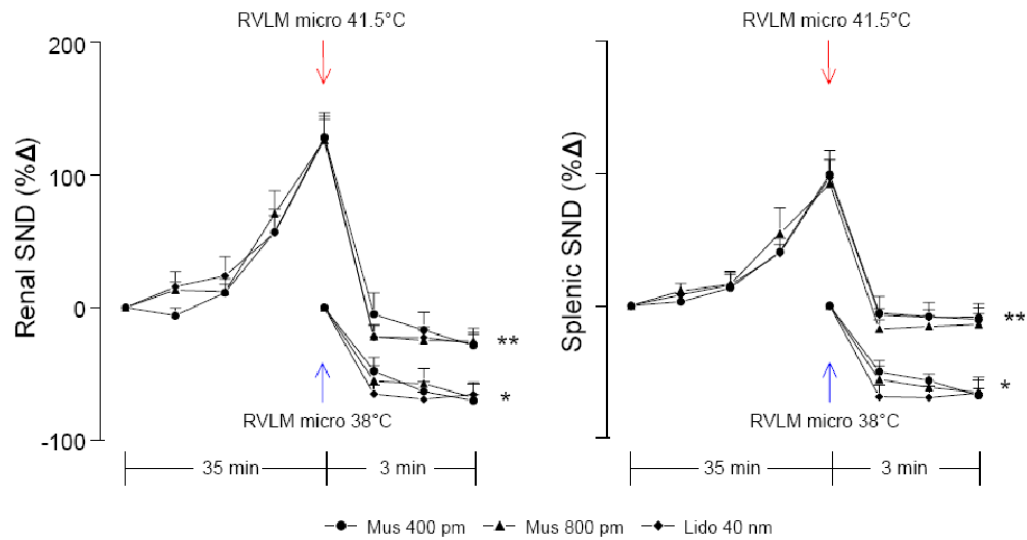


Figure 5.

Changes in renal and splenic SND from RVL microinjection experiments completed at 41.5°C (red arrows) and RVL microinjection experiments completed at 38°C (blue arrows). *RVLM muscimol (400 and 800 pmol) and lidocaine (40 nmol) microinjections at 38°C significantly different from control at 1, 2, and 3 min post-microinjection. **RVLM muscimol (400 and 800 pmol) and lidocaine (40 nmol) microinjections significantly different from peak-heating levels (41.5°C) at 1, 2 and 3 min post-microinjection.

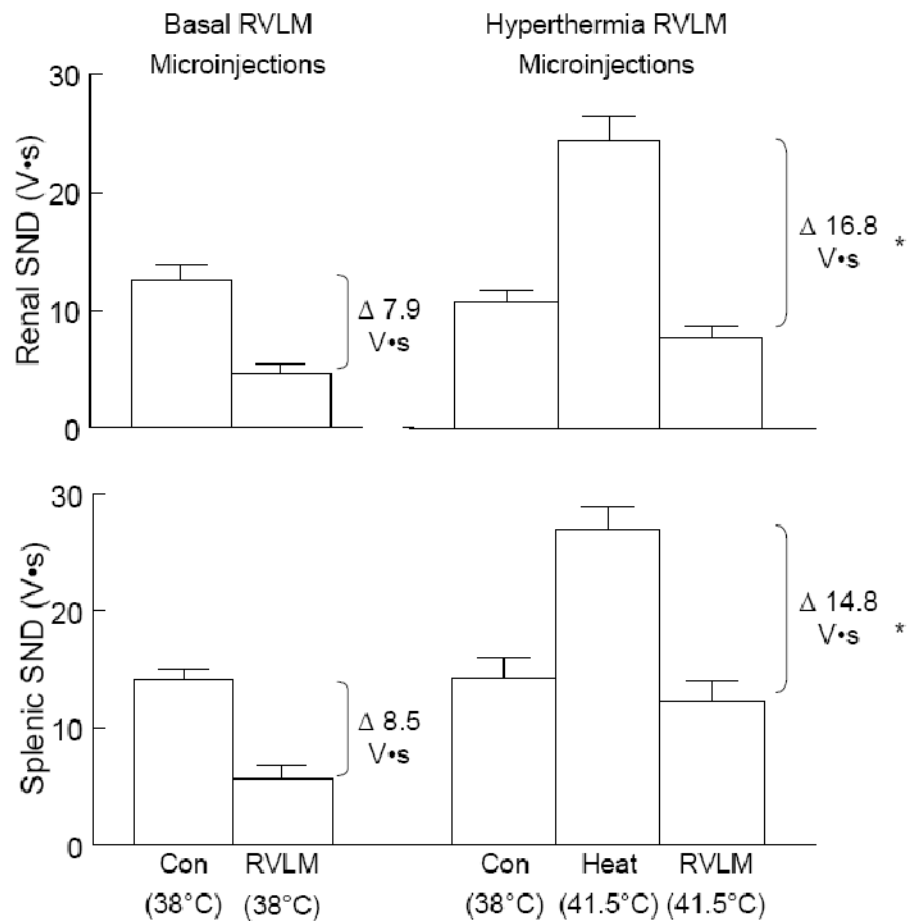


Figure 6. Changes in the absolute level of renal and splenic SND (recorded as volt•seconds) following RVLM microinjections of muscimol (400 and 800 pmol) and lidocaine (40 nmol) (data combined for presentation) from experiments with Tc maintained at 38°C (left panels) compared to experiments in which Tc was increased to 41.5°C (right panels). *Change in SND (V•s) significantly different following RVLM microinjection of muscimol (400 and 800 pmol) and lidocaine at 41.5°C compared to RVLM microinjection of muscimol (both doses) and lidocaine at 38°C

Table 1
Changes in renal and splenic SND 3 minutes after RVLM microinjections of muscimol (Mus, 400 and 800 pmol) and lidocaine (40 nmol) at 41.5°C in baroreceptor-intact and sinoaortic denervated (SAD) rats

		Intact Recovery (3 min post)	SAD Recovery (3 min post)
Renal SND (%Δ)			
	Mus 400	-25±16	-31 ±22
	Mus 800	-17±8	-32±11
	Lidocaine	-28±9	-26±11
Splenic SND (%Δ)			
	Mus 400	-11±21	-8±22
	Mus 800	-7±9	-18±13
	Lidocaine	5±5	-19±10